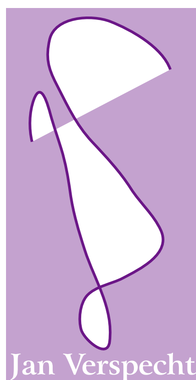

Jan Verspecht bvba

Mechelstraat 17
B-1745 Opwijk
Belgium

email: contact@janverspecht.com
web: http://www.janverspecht.com

Large-Signal Network Analysis

Jan Verspecht

IEEE Microwave Magazine, Vol. 6, Issue 4, December 2005, pp. 82-92

© 2005 IEEE. Personal use of this material is permitted. However, permission to reprint/republish this material for advertising or promotional purposes or for creating new collective works for resale or redistribution to servers or lists, or to reuse any copyrighted component of this work in other works must be obtained from the IEEE.

IEEE
microwave
for the Microwave & Wireless Engineer
MAGAZINE
Volume 6 • Number 4 • December 2005

S-Parameter Measurement

- Multiport VNA Measurement
- Large-Signal S-Parameters

IEEE microwave
for the Microwave & Wireless Engineer MAGAZINE

Volume 6 • Number 4 • December 2005 • ISSN 1527-3342

IEEE Microwave Theory and Techniques Society

Editor
Madhu S. Gupta
San Diego State University
5500 Campanile Drive
San Diego, CA 92182-1309 USA
+1 619 594 7015
microwave.editor@ieee.org

Features Associate Editors
William D. Jemison
Lafayette College
Dept. Electrical & Computer Engr.
Easton, PA 18042 USA
+1 610 330 5425
w.d.jemison@ieee.org

Ed Ackerman
Photonic Systems, Inc.
103 Terrace Hall, Suite A
Burlington, MA 01803 USA
+1 978 670 4990, ext. 227
eackerman@photonicsinc.com

Application Notes Associate Editor
Inder Bahl
M/A-COM Inc.
5310 Valley Park Dr.
Roanoke, VA 24019 USA
+1 540 563 8638
inderb@tycoelectronics.com

IEEE Periodicals Magazines Department
445 Hoes Lane, Piscataway, NJ 08854
+1 732 562 3950, fax +1 732 981 1855
Web http://www.ieee.org/magazines

Patrick Gibbons, *Managing Editor*
Janet Dudar, *Art Director*
Gail A. Schnitzer, *Assistant Art Director*
Cathline Tanis, *Senior Ad Production Coordinator*
Robert Smrek, *Production Director*
Dawn M. Melley, *Editorial Director*
Fran Zappulla, *Staff Director*

Advertising Sales
Susan Schneiderman, *Business Development Manager*
+1 732 562 3946, fax +1 732 981 1855

features

72 **Multiport Vector Network Analyzer Measurements**
Hardware architectures and calibration procedures for multiport measurements and their impacts on flexibility and uncertainties.
J. Martens, D. Judge, and J. Bigelow

82 **Large-Signal Network Analysis**
An invitation to join the rapidly growing LSNA community that is improving microwave measurements and is on its way to building a multimillion dollar business.
Jan Verspecht

application notes

94 **A Potentially Significant On-Wafer High-Frequency Measurement Calibration Error**
James C. Rautio and Robert Groves

on the cover:

© ARTVILLE

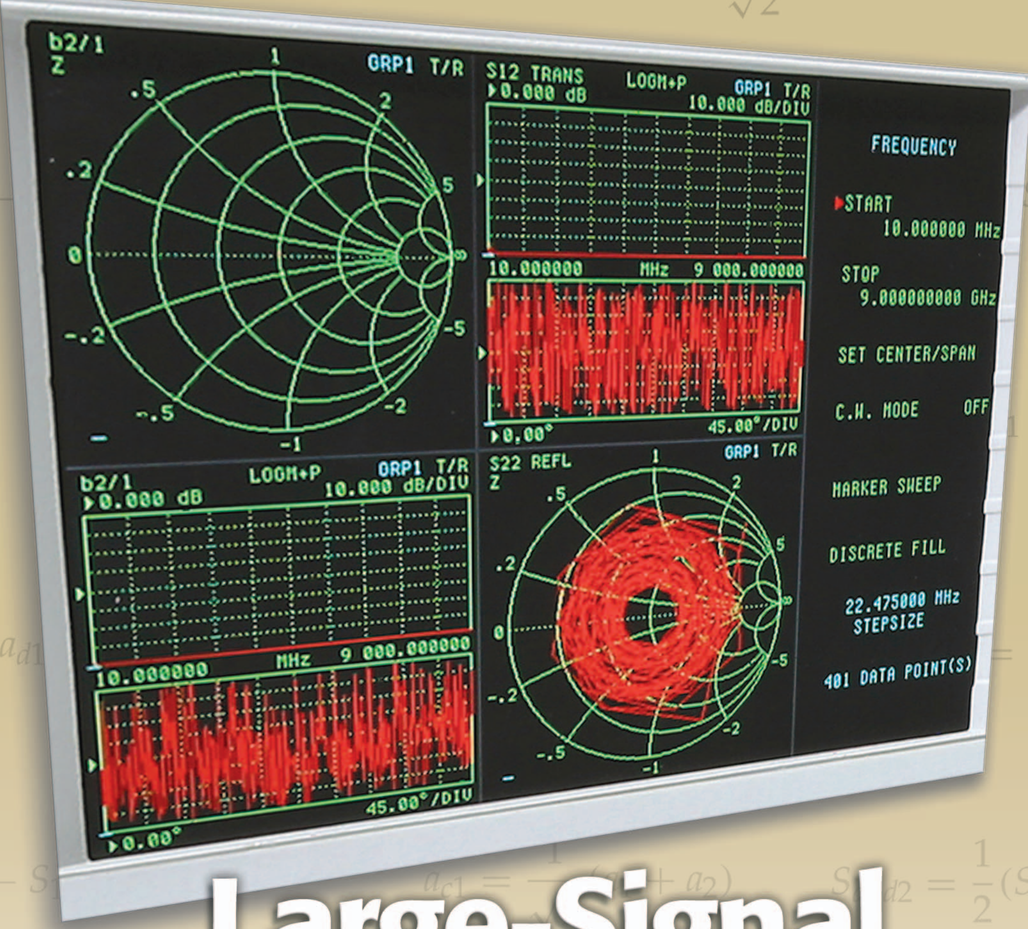

Large-Signal Network Analysis

Jan Verspecht

According to Mike McKinley of Georgia Tech, it's "the Holy Grail of microwave instrumentation and measurements," it's "a new measurement science," according to Don DeGroot of Connected Community Networks and "an enabling path to taking nonlinear models to a higher level of fidelity and value," says Larry Dunleavy of Modelithics.

I prefer to call it large-signal network analysis (LSNA). Today, LSNA is undoubtedly still in its infancy. A small community knows about the theoretical concepts, and a happy few have access to LSNA hardware. This community is growing rapidly, however, and I have no doubt that the people of this community will soon revolutionize the microwave measurement business as profoundly as S-parameter technology did in the 1980s. I hope with this article to inspire you to join this rapidly growing LSNA community that is improving microwave measurements and is on its way to building a multimillion dollar business.

Background

Unlike cellophane or penicillin, LSNA technology was not invented by accident or by a flash of genius. Instead, it resulted from first recognizing a real problem faced by microwave designers

Jan Verspecht (contact@janverspecht.com) is with Jan Verspecht bvba in Steenhuffel, Belgium.

 1527-3342/05/$20.00©2005 IEEE

and then carefully fashioning a solution for it. The real problem I am referring to is the gap between results that can be generated via computer-aided design (CAD) tools and those that can be measured with current microwave instrumentation.

A classic vector network analyzer (VNA) can automatically characterize all kinds of microwave components by measuring S-parameters. These S-parameter data can be made directly accessible to the designers in a CAD environment, where the simulated device behavior accurately represents the measured device behavior. Alternatively, a manufactured component can easily be verified against design specifications by measuring its S-parameters. In other words, a classic VNA provides a consistency check between the actual physical device and the mathematical abstraction that resides inside the simulator. The result is a very efficient design cycle. If this works so great, why, then, do we need LSNA?

The answer is that S-parameters are based on a superposition principle and, therefore, can only accurately represent linear devices, like filters, cables, couplers, and connectors, whose behavior is determined solely by the linear Maxwell's equations. How about all those S-parameter measurements of semiconductor amplifiers? There is certainly more than the linear Maxwell's equations in there. Does this mean that S-parameter measurements of amplifiers (which all exhibit nonlinearity) are questionable?

The answer is "yes." Such measured data is questionable without a verification whether the applied signal levels during the S-parameter measurement are small enough to justify the superposition principle. This is typically done by measuring the S-parameters at two different power levels and by verifying that the resulting curves are identical. So, we ensure that the applied amplifier stimulus is small enough to verify that the superposition principle was valid when we measure the S-parameters of a semiconductor amplifier. Are we happy now?

The answer is, unfortunately, "no." Although the measured S-parameters for the amplifier are valid and accurate, they still can only be used to predict the behavior for a small signal stimulus. The measured S-parameters can not predict the behavior of the amplifier whenever the amplitude of the stimulus becomes significant compared to the operating range of the device. Whenever the behavior deviates from the superposition principle, people say that the component introduces nonlinear distortion effects. These effects are usually categorized as compression, amplitude modulation–phase modulation (AM-PM) conversion, and harmonic and intermodulation product generation.

History

To the best of my knowledge, the history of LSNA technology started in October 1988. That month, the IEEE published the paper "High-Frequency Periodic Time-Domain Waveform Measurement System," by Sipilä et al. [2]. The paper reported on the first measurement setup that had the two necessary ingredients of LSNA technology:

- a unified approach for the frequency and the time domain
- the availability of wave as well as a voltage-current representations.

Sipilä et al. used a two-channel 14-GHz oscilloscope and one coupler to measure the voltage and current waveforms at the gate and drain of a HF transistor.

In 1989, Lott reported on a system based exclusively on a VNA test set and receiver [14]. He measured the harmonics with the receiver by tuning it consecutively to each of the harmonics. An ingenious phase reference method is used to align the harmonic phases (the so-called golden diode approach).

In 1990, Kompa and Van Raay reported on a similar setup based on a two-channel microwave oscilloscope combined with a complete VNA test set and receiver [15]. The receiver is used to measure the fundamental data, the oscilloscope is used for the harmonics.

A breakthrough took place in 1992 with the commercial introduction of the Hewlett-Packard microwave transition analyzer (MTA). This two-channel receiver has a bandwidth of 40 GHz and directly measures phase and amplitude of fundamental and harmonic spectral components. It was first used by Kompa and Van Raay [16]. From 1994 on, it was also used by Demmler, Tasker, and Schlechtweg [17]; Leckey [18]; and Wei and Tkachenko [19].

In 1995, my colleagues and I started using two synchronized MTAs as a four-channel harmonic receiver [20]. This work was performed at the lab of Prof. Barel of the Vrije Universiteit Brussel and resulted in the first prototype of the nonlinear network measurement system, later to be called the *large signal network analyzer*. A picture of such a system is shown in Figure 1.

In 2000, Arnaud and her colleagues built an LSNA system based on a modified VNA receiver with load-pull and pulsed measurement capability at the IRCOM in France [21]. She uses a phase reference similar to Urs Lott. The same year, I added envelope domain capability to our LSNA prototype instrument [22].

LSNA Metrology

Building an LSNA instrument is one thing, making sure that the measurements are accurate and that the calibration procedures are traceable to national standards is yet another technological challenge. Inevitably, all of the LSNA microwave and RF hardware components introduce significant linear distortions. These distortions have to be eliminated by using calibration procedures that are extended versions of the calibration procedures used for classic VNAs.

Calibration Procedure Basics

Before continuing with the calibration aspects, it is useful to consider the hardware schematic of an LSNA (see Figure 2). During an experiment, you want to measure the phases and amplitudes of a discrete set of spectral components at the DUT signal ports. Let us call these quantities the *DUT quantities* and denote them by $D1$ and $D2$, where the number refers to the test port. Unfortunately, we do not have direct access to these quantities. The only information we can get are the uncalibrated measured values. These are called the *raw quantities* and are denoted by $R1$ and $R2$. All calibration procedures are based on an error model. The main assumption we will use for our error model is that there exists a linear relationship between the raw measured spectral components and the actual spectral components at the DUT signal ports. In order for this assumption to be valid, it is necessary to avoid any nonlinear distortions in the LSNA signal receiver itself. Programmable attenuators are used for that purpose. By limiting the peak amplitude at the input of the frequency convertor to about 100 mV, a spurious free dynamic range of 65 dB is achieved. The linear error model can be described by the following matrix equation:

$$\begin{bmatrix} a_h^{D1} \\ b_h^{D1} \\ a_h^{D2} \\ b_h^{D2} \end{bmatrix} = K_h e^{j\phi_h} \begin{bmatrix} 1 & p_h & 0 & 0 \\ q_h & r_h & 0 & 0 \\ 0 & 0 & s_h & t_h \\ 0 & 0 & u_h & V_h \end{bmatrix} \begin{bmatrix} a_h^{R1} \\ b_h^{R1} \\ a_h^{R2} \\ b_h^{R2} \end{bmatrix}. \quad (3)$$

Note that h refers to the harmonic index of a tone. The RF correction is described by a set of 16-element matrices (one for each harmonic). Note that eight zeros are present. This corresponds to the assumption that there is no cross-coupling between Port 1 and Port 2 of the instrument. The goal of the RF calibration is to determine the elements of this matrix. This goal is achieved in three steps: a classical VNA calibration to determine the seven coefficients p_h, q_h, r_h, s_h, t_h, u_h and v_h; an amplitude calibration to determine K_h; and a harmonic phase calibration to determine the unit length phasors $e^{j\phi_h}$.

For a coaxial DUT, the amplitude and the harmonic phase calibration are performed by connecting a power sensor and a harmonic phase reference generator (HPR) directly to the LSNA test ports. A HPR is a source that produces a calibrated harmonic spectrum of com-

It is the goal of LSNA technology to go beyond S-parameters to provide a tool set that may be used to accurately characterize nonlinear components, such as amplifiers, under large-signal excitation. This is achieved by designing instruments that can accurately and completely characterize devices under realistic large-signal operating conditions and developing software that can accurately represent the measured nonlinear device behavior in a simulator.

Theoretical Foundations

LSNA technology is empowered by a unique combination of two mathematical transformations. The first one is the transformation between a traveling voltage-wave formalism and a voltage-current representation. The second one is the transformation between the time domain and the frequency domain. Classic instrumentation tools do not readily combine both transformations. The S-parameter data of a classic VNA, for example, is rarely studied in a time-domain representation of voltages and currents. LSNA technology enables one to easily study the data in either domain (time or frequency) and in either representation (waves or voltage-current). As will be demonstrated later, such a combination is necessary to get insight into large-signal behavior of nonlinear components.

Waves Versus Voltage Current

Let us start with the transformation between a wave formalism and a voltage-current representation. S-parameters are defined as a ratio between traveling voltage waves, where the letter A refers to the incident waves and the letter B refers to the scattered waves. The use of wave quantities is native to classic VNAs, which measure the ratio of the incident and scattered waves. It is important to note that, under the superposition assumption required for classic vector network analysis, the stimulus frequency will be the only frequency present, there will be no new frequencies (e.g., harmonics or intermodulation distortion products) present. An LSNA instrument will measure A and B waves at the terminals of a device under large-signal operating conditions. Since a ratio is not sufficient to describe nonlinear behavior, an LSNA instrument will measure the absolute values of all wave quantities (including harmonics and intermodulation distortion products) and not merely their ratios. On the simulator side, a power amplifier designer will often simulate and

ponents. The power sensor and HPR can be considered additional connectorized calibration elements, just like a load, a short, or an open calibration element. Note that, unlike the HPR calibration, the power calibration is performed by applying one tone at a time since the power sensor is not frequency selective. The HPR and power sensor measurements cannot directly be done, however, for an on-wafer measurement since both the HPR and the power sensor have a coaxial output connector. The solution to this problem is based on the use of the reciprocity principle between the probe tip and the generator input connector of the test set. The harmonic phase reference generator and the power sensor are connected to this coaxial input port, and the final measured characteristic can be transformed to the probe tip based on the fact that the test set is reciprocal. This transformation does require an additional load-open-short calibration at the generator input connector. During all of the above measurements, the probe tips are connected to a line calibration element.

The Harmonic Phase Reference Generator

An HPR generates fundamental harmonics with a stable and very well characterized phase relationship. The main components of the HPR are a power amplifier, a step-recovery diode, and a pulse-sharpening nonlinear transmission line (together with cables and padding attenuators). Developing a traceable calibration procedure for the HPR was the most challenging aspect of the LSNA calibration.

The HPR is characterized by using a broadband sampling oscilloscope. A discrete Fourier transformation returns the phase relationship between all of the relevant harmonics (up to 50 GHz). Note that the HPR needs to be characterized across a whole range of fundamental frequencies with enough resolution to allow interpolation. Our HPR covered one octave of fundamental frequencies, from 600 up to 1,200 MHz. The HPR is a stable device, such that it is sufficient to recalibrate it with an oscilloscope measurement about once every year.

The accuracy of the HPR characterization is, in turn, determined by the accuracy of the sampling oscilloscope measurement. The sampling oscilloscope introduces linear distortions that can be characterized by the so-called nose-to-nose calibration procedure, which was invented by Rush at Hewlett-Packard in 1989 [4]. I performed extensive research on the accuracy of the nose-to-nose calibration procedure as part of my Ph.D. work and later, at the National Institute of Standards and Technology (NIST), Remley and her colleagues [23] performed it. The research at the NIST resulted in a very accurate harmonic phase standard based on a broadband (110 GHz) electro-optic sampler setup [5].

analyze the voltage and current waveforms at the terminals of a power transistor. An LSNA instrument must be able to convert the measured wave (noted *AB*) behavior of a component into a voltage-current (noted *VI*) representation. A good understanding of the device behavior is often only possible by taking a look at both kinds of signal representations. The relationships between the *VI* and the *AB* quantities are given by simple algebraic equations:

$$A = \frac{V + Z_c I}{2} \qquad B = \frac{V - Z_c I}{2} \tag{1}$$

and

$$V = A + B \qquad I = \frac{A - B}{Z_c}. \tag{2}$$

Z_c is the characteristic impedance associated with the wave formalism. By convention, most of todays instrumentation uses a Z_c equal to 50 Ω. These simple equations are based on the famous telegraphers equation. Please be aware that other wave definitions are in use. Valuable information on the scientific foundation of wave formalisms can be found in [1].

Time Domain Versus Frequency Domain

The second transformation relates to the time domain and the frequency domain. A power amplifier designer will typically want to visualize voltage and current waveforms as they appear at the terminals of a power transistor in the time domain. An LSNA instrument typically measures the spectral components of the *A* and *B* waves. Since the *A* and *B* waves contain harmonics and intermodulation distortion (IMD) products, in addition to the fundamental frequency, the transformation between the time and the frequency domain can be performed only if the amplitude of all spectral components and the cross-frequency phase relationship between the spectral components are measured. Cross-frequency means that it is not sufficient to determine the phase relationship between spectral components with equal frequencies, as it is the case with S-parameters, but one needs to measure the phase relationship between components that have different frequencies (like a fundamental and harmonics or like different intermodulation products). Spectral component phase information is undoubtedly the most important ingredient in going from classic approaches to an LSNA approach since it enables measurements to

be represented in the time as well as frequency domain. Because of this fact, time domain gurus often refer to an LSNA instrument as a "calibrated oscilloscope with voltage and current probe."

Envelope Domain

Next to the pure time and frequency domain, many engineers represent their signal as a spectrum that varies over time. This kind of representation is useful if the signals are modulated carriers, as is the case for most wireless telecommunication applications. Signals resulting from both analog and digital modulation schemes can be represented as so called complex envelopes. A complex envelope is a complex time function where the real part represents the in-phase component and the imaginary component represents the quadrature component of a modulated carrier. The in-phase component is usually called *I,* and the quadrature component is usually called *Q*. This *IQ* or envelope representation is not only used by engineers but is also used inside advanced envelope domain simulators. The concept is also native to instrumentation like the vector signal analyzers (VSAs) and digital modulation synthesizers. An LSNA instrument is able to construct these envelope representations of the measured *A* and *B* waves and can, as such, also perform typical VSA measurements.

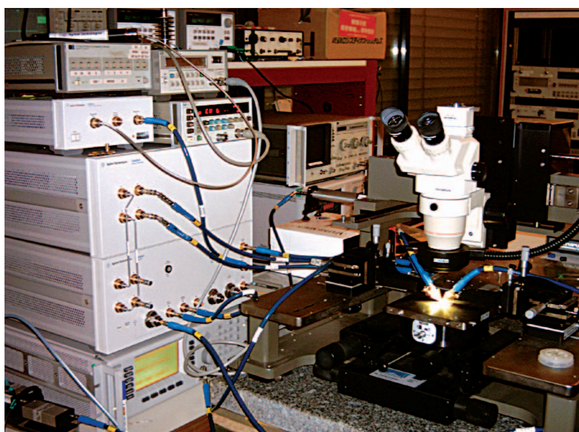

Figure 1. *Picture of the LSNA at IRCOM (France).*

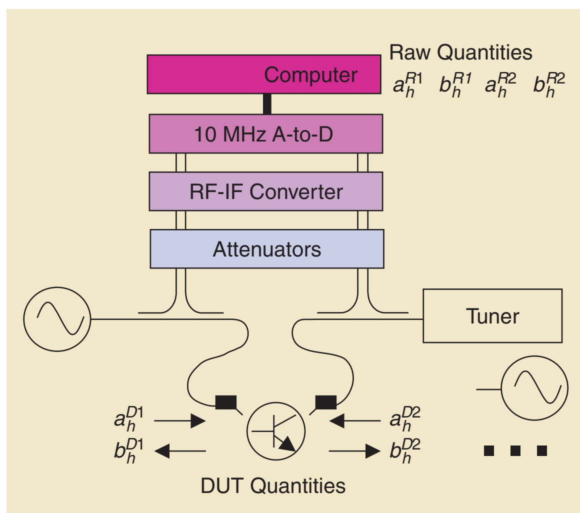

Figure 2. *LSNA architecture.*

LSNA Hardware

The combination of the simple yet powerful concepts of the wave versus voltage-current formalism and the time to frequency domain transformation are not present with a single classic instrument like a VNA, VSA, oscilloscope, or spectrum analyzer. In many cases, many separate measurements are being performed using several classic microwave instruments. A VNA is used to characterize the small-signal matching characteristics, a VSA is used to characterize the distortion of the complex envelope of a signal, a spectrum analyzer is used to take a look at the harmonic power, and an oscilloscope is used to look at time-domain waveforms. In contrast to classic instrumentation, an LSNA instrument provides one measurement tool that measures all of the aforementioned characteristics in a consistent and accurate way. In the following, I explain the architecture of the large-signal network analyzer instrument as my colleagues and I developed it while working for the Hewlett-Packard company (later to become Agilent Technologies). A picture of such a system is shown in Figure 1.

LSNA Hardware Architecture Overview

The hardware architecture of the LSNA, illustrated in Figure 2, is relatively simple. Four couplers are used for sensing the spectral components of the incident and scattered voltage waves at both device-under-test (DUT) signal ports. The sensed signals are attenuated to an acceptable level before being sent to the input channels of a four-channel broadband RF–IF converter. This RF-IF converter operates based on the harmonic sampling principle (to be described in more detail in the next section) and converts all of the spectral components coherently to a lower frequency copy (below 4 MHz). The resulting IF signals are digitized by a set of four high-performance analog-to-digital converters (ADCs). A computer does all the processing needed to transform the calibrated data into one of the three formats (*AB* or *VI*, time, frequency, or envelope domain).

The primary specifications of the LSNA prototype, as it was developed by our research group, are as follows: the calibrated RF frequency range equals 600 MHz to 50 GHz, the maximum RF power equals 10 W, and the maximum bandwidth of the modulated signal equals 8 MHz. The repetition frequency of the modulation is typically a few kilohertz. Note that synthesizers and tuners for the signal generation can be (and usually are) added externally. They are not considered part of the LSNA. Although not shown here for reasons of simplicity, dc bias circuitry is also present.

Harmonic Sampling

The four-channel RF–IF sampling frequency converter, illustrated in Figure 3, is the core of the LSNA. It is based on broadband sampler technology. One digital synthesizer drives four sampler switches at a rate close to 20 MHz. This rate is called the *local oscillator (LO) frequency* (f_{LO}). Each time the switch closes for a duration of about 10 ps, it samples a little bit of charge and sends it to a low-pass filter. When the synthesizer frequency is properly chosen, a low-frequency copy of all input spectral components at the output of the filter is found.

The harmonic sampling idea is illustrated in Figure 4. It corresponds to the case where one has a fundamental tone and harmonics. Assume that we need to measure a 1-GHz fundamental together with its second and third harmonic. We choose a LO signal having a frequency of 19.98 MHz. The 50th harmonic of the LO will have a frequency of 999 MHz. This component mixes with the fundamental and results in a 1-MHz mixing product at the output of the converter. The 100th harmonic of the LO has a frequency of 1998 MHz, mixes with the second harmonic at 2 GHz, and results in a 2-MHz mixing product. The 150th harmonic of the LO has a frequency of 2,997 MHz, mixes with the third harmonic at 3 GHz, and results in a 3-MHz mixing product. The final result at the output of the converter is a 1-MHz fundamental together with its second and third harmonic. This is actually a low-frequency copy of the high-frequency RF signal. This signal is then digitized, and the values of the spectral components are extracted by applying a discrete Fourier transformation.

Although based on the same principles, the process for a modulated signal is more involved. After the RF–IF conversion, all harmonics and modulation tones can be found back in the IF channel, ready for digitizing and processing. The technique is described in detail in [3].

Applications

The following gives an overview of the many applications based on the LSNA concepts. Practical examples are presented covering a whole spectrum of applications, including transistor characterization, loadpull waveform engineering, frequency-domain black-box modeling, state-space black-box modeling techniques, active digital-signal integrity measurements, and spectral regrowth measurements.

Waveform Measurements

As explained above, the LSNA measures both the amplitude and the phase of all significant harmonics of both the incident and the scattered traveling voltage waves. Applying an inverse Fourier transform results in corresponding time-domain waveforms. The time-domain traveling voltage waves can be transformed into a current and a voltage waveform. In the time-domain current-voltage visualization mode, the LSNA emulates a broadband oscilloscope having calibrated voltage and current probes. Such information can be very valuable to get a unique insight into issues (e.g., transistor reliability) that are often related to hard nonlinear phenomena.

Unlike cellophane or penicillin, LSNA technology was not invented by accident or by a flash of genius.

In Figure 5, we plot the voltage and current time domain waveforms as they appear at the gate and drain of a microwave field-effect transistor (FET). These measurements are performed while applying an excitation signal of 1 GHz at the gate. The signal amplitude is increased until we see a so-called breakdown current. It shows up as a negative peak (20 mA) for the gate current and as an equal amplitude positive peak at

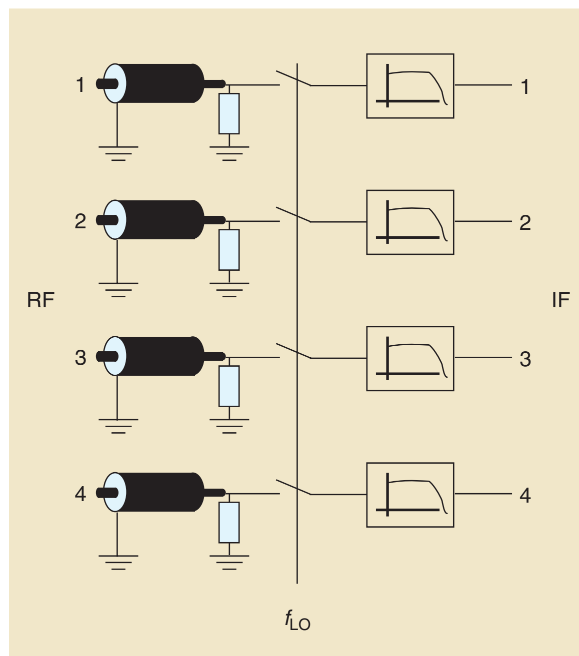

Figure 3. *Sampling frequency convertor.*

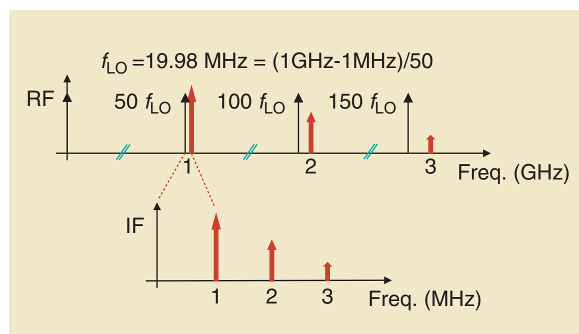

Figure 4. *Sampling a fundamental tone with harmonics.*

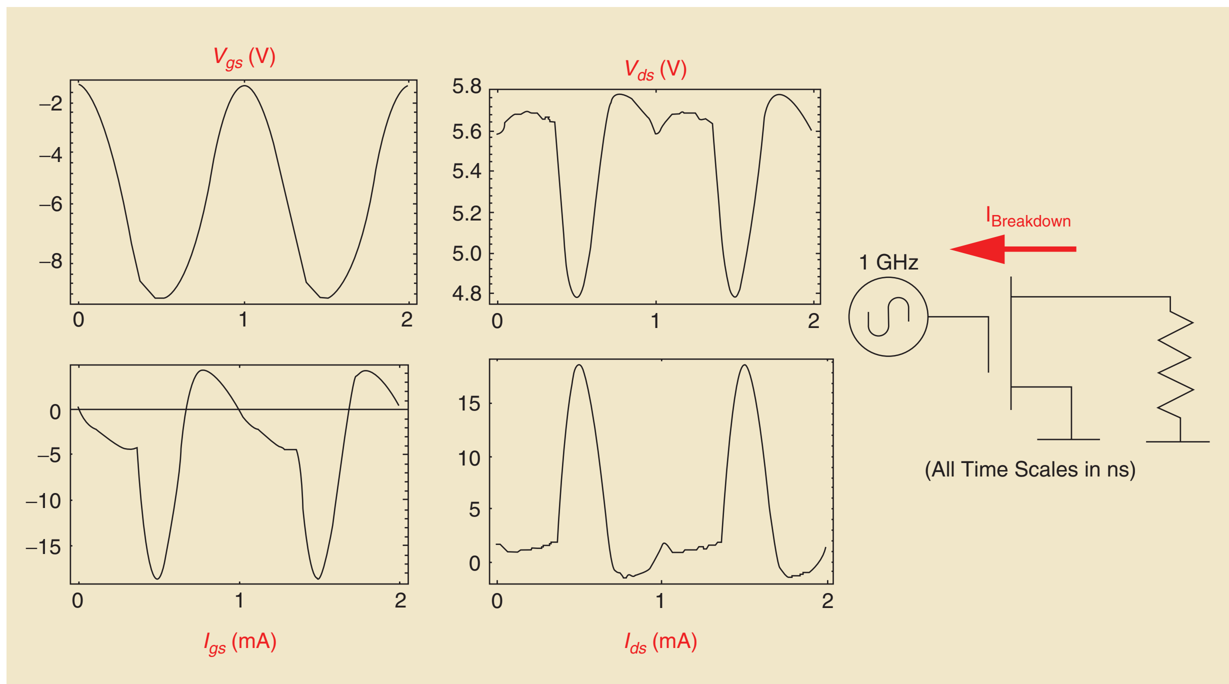

Figure 5. *Breakdown currents.*

the drain. Using the LSNA, we can actually witness the breakdown current that flows from the drain towards the gate. This kind of operating condition deteriorates the transistor and is a typical cause of transistor failure. To our knowledge, these measurements are the first ever performed of breakdown current under large-signal RF excitation [6].

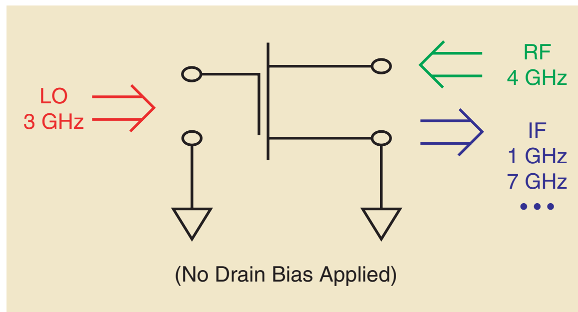

Figure 6. *Resistive mixer schematic.*

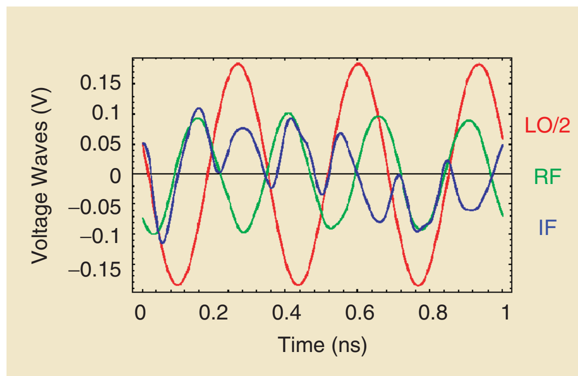

Figure 7. *Resistive mixer time domain waveforms.*

Another example is the usage of a high-electron mobility transistor (HEMT) transistor in a resistive mixer configuration [7]. The schematic of the mixer is shown in Figure 6. A large LO signal is driving the gate. This causes the drain of the transistor to behave as a time-dependent switch. The switch is toggled at the rate of the LO (in our example, 3 GHz). Any incident voltage wave at the drain (in our example, 4 GHz) experiences a fast time-varying reflection coefficient (toggling at a 3 GHz rate). The voltage wave reflected from the drain will, thus, be equal to the incident wave multiplied by the time-varying reflection coefficient. The scattered wave contains the primary mixing products (1 and 7 GHz) of the LO and the incident RF signal. The working principle is nicely demonstrated by looking at the measured time-domain representation of the voltage waves. Figure 7 illustrates how the incident wave (RF) and reflected wave (IF) are in phase or in opposite phase, depending on the instantaneous amplitude of the LO. For a high LO, the RF experiences a low drain impedance and behaves like a short corresponding to a reflection coefficient close to -1 (reflection in opposite phase); for a low LO, the RF experiences a high drain impedance and behaves like an open corresponding to a reflection coefficient close to $+1$ (reflection in phase). Note that a 1- and a 7-GHz component in the resulting reflected wave (IF) can be clearly distinguished. For clarity, the amplitude of the LO signal on Figure 7 has been divided by two.

Another interesting application is the calibrated on-wafer measurement of high-speed digital signals [8]. The classic technique for performing such measurements makes use of a microwave oscilloscope. The

cables, connectors, and probes that are used to connect the oscilloscope to the wafer introduce significant distortions in the measurement of the eye-diagrams of digital signals. Performing similar measurements with an LSNA results in fully error-corrected waveforms all the way up to the tip of the probe. In Figure 8, it is clear that the oscilloscope data lacks certain details like offset and overshoot when compared to the calibrated LSNA data. This is due to dispersion of the oscilloscope cables as well as to the presence of jitter on the timebase of the oscilloscope. Both of these distortions are also present with the LSNA frequency converter but are compensated with VNA-like accuracy by the LSNA calibration procedure.

A last application of waveform measurements is power amplifier design by applying waveform engineering [9]. With waveform engineering, different harmonic impedances at the DUT signal ports are applied, and specific performance parameters, like power-added-efficiency (PAE), are optimized by looking at the voltage and current waveforms. This is illustrated in Figure 9. Traditionally, current and voltage waveforms are not readily available from measurements, so the method is usually applied only in a simulator. The problem with using simulators is that the accuracy of the final result will depend heavily on the quality of the large-signal transistor model.

Connecting a harmonic tuner to the test set of the LSNA makes it possible to apply the method in real life, without the need of a simulator or transistor model.

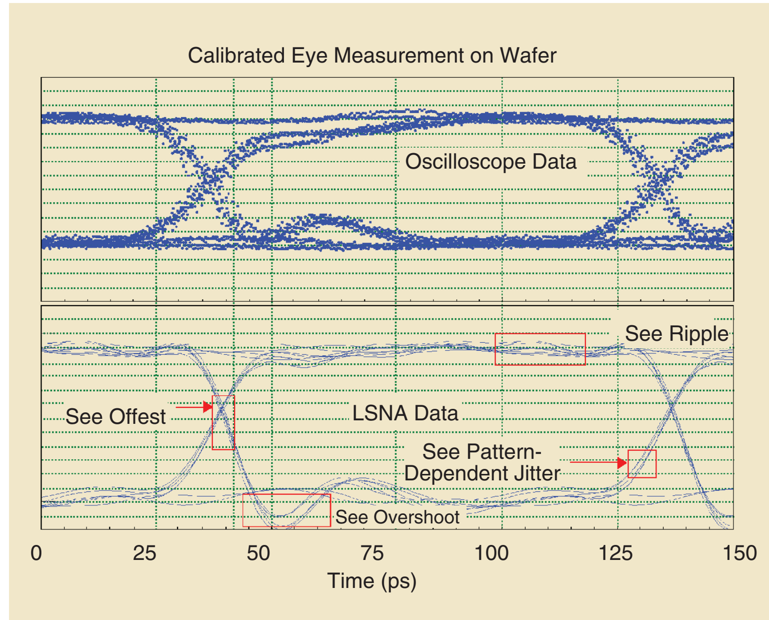

Figure 8. *Measuring digital signals.*

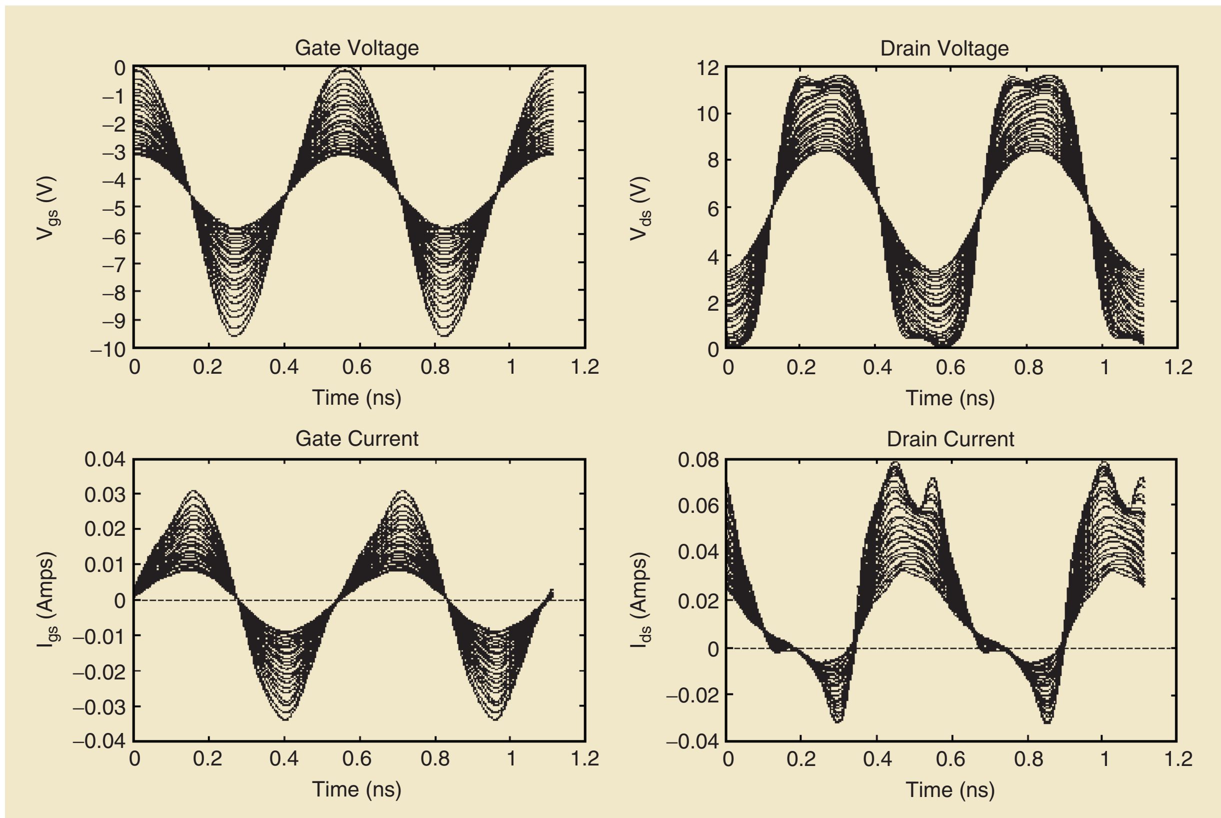

Figure 9. *Harmonic loadpull voltage and current waveforms.*

Using the combination of an LSNA with a tuner and using the waveform engineering technique, Nébus et al. could demonstrate an increase of the PAE of a metal semiconductor FET (MESFET) Class F amplifier from 50% to a record 84% [9].

LSNA technology is empowered by a unique combination of two mathematical transformations.

Transistor Modeling

Next, we will show how the LSNA data can be used in advanced physical transistor modeling. By physical models, we refer to electrical circuit schematics containing nonlinear capacitors, voltage-controlled current sources, and resistors. All nonlinear elements are typically defined by means of analytical functions, which are often derived from the physical description of the transistor (geometry and semiconductor doping profile). These models can have more than 100 parameters that need to be determined. Examples of such models are BSIM3, Chalmers, and Materka. The approach of optimizing existing physical models using the LSNA is pretty straightforward [10]. First, a set of LSNA experiments is performed that covers the operating range of the transistor. This data is imported into a simulator. The measured incident voltage waves are applied to the model in the simulator. The model parameters are then found by tuning them such that the difference between the measured and modeled scattered voltage waves is minimized. Note that one can often use built-in optimizers for this purpose. As with all nonlinear optimizations, it is necessary to have reasonable starting values (these can be given by a simplified version of the classical approaches).

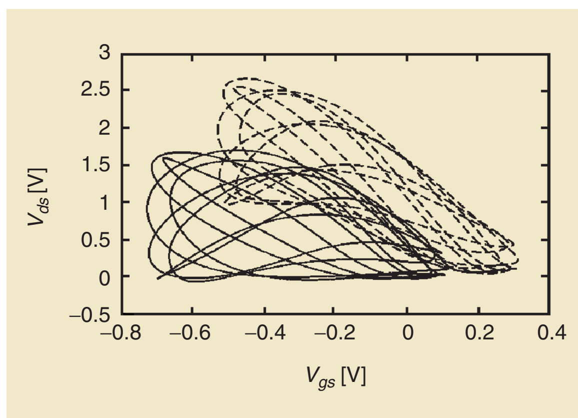

Figure 10. *Covering of the FET drain and gate voltage state-space using a two-tone.*

A recent and upcoming transistor-modeling approach is based on state-space models [11]. These models are black-box time-domain models that are typically used in physics for describing all kinds of nonlinear dynamical processes. A first microwave transistor model of this kind is the so-called Root-model. It is a simple version of the more general state-space function model. It was originally invented by David Root. For a Root-model, the model parameter extraction is

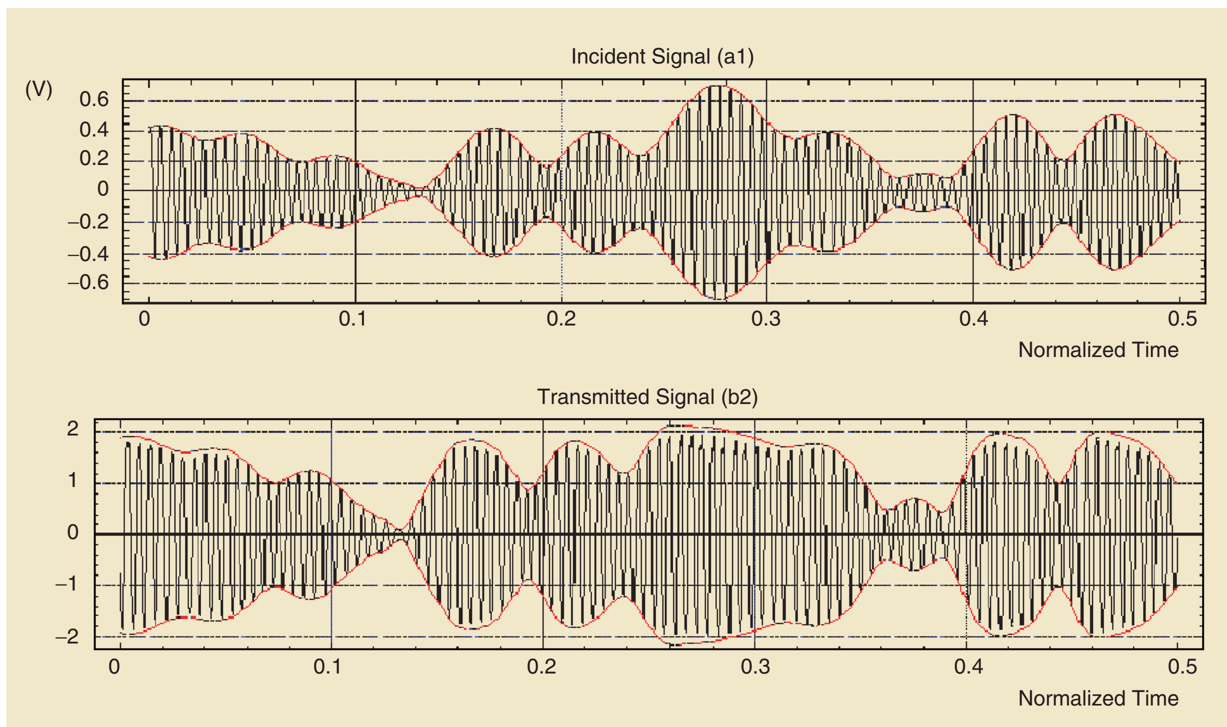

Figure 11. *Measured time domain waveforms.*

based on bias-dependent S-parameter measurements. In a state-space function approach, one assumes that the port currents of a device are a general nonlinear function of a limited set of state variables. The state variables are the port voltages, the first- and higher-order derivatives of the port voltages, and the first- and higher-order derivatives of the port currents. One can identify the relevant set of state variables and the functions themselves by performing sufficient LSNA experiments and by processing the gathered data. The state-space models are technology independent and can be applied to all nonlinear microwave circuits as long as they do not contain distributed elements. Examples are single transistors or small RFICs. As soon as distributed elements are present, the set of relevant state-space variables becomes excessively large (in theory, an infinite number) and the state-space functions can no longer be practically identified. One of the main challenges is the experiment design. In order to have a good fit to the state-space functions, it is necessary to have a dense coverage of the state-space over a meaningful range. An original solution to this was developed by Schreurs [12]. She simultaneously applied excitation tones having different frequencies to the gate and the drain of a microwave transistor. The two frequencies used were 4.2 and 4.8 GHz. Note that both frequencies are integer multiples of 600 MHz, which implies that a single-frequency grid of 600 MHz is sufficient for the LSNA data acquisition. Figure 10 illustrates the resulting coverage of the state-space corresponding to two measurements (two different bias settings are applied). The two-tone experiment allows dense coverage of the gate and drain voltage state-space over a meaningful range. It might be interesting to note that the two-tone technique was actually invented several decades ago by mechanical engineers dealing with the characterization of nonlinear mechanical structures.

Scattering Functions

While the LSNA can improve measurement capability for the traditional measurements described here, I have no doubt that the breakthrough of LSNA technology will come from the ability to measure scattering functions [13], [24], [25]. This is a black-box, frequency-domain modeling technique. The approach is an extension of S-parameters towards large-signal behavior. Ideally, one connects a DUT to an LSNA instrument, and a model is automatically extracted that accurately describes all kinds of nonlinear behavior, such as amplitude and phase of harmonics, compression characteristics, AM-PM, spectral regrowth, amplitude-dependent input, and output match. A simple measurement example is given in Figure 11. It shows the measured incident and transmitted wave at the input and, respectively, output terminals of an RFIC. The applied signal was carefully designed to have characteristics that are very similar to the signals that are to be used for the final application [in this case, a code division, multiple-access (CDMA) signal with a 1.9-GHz carrier]. Note the use of the normalized time scale. In order to visualize the distortion throughout the envelope, the envelope time scale and the actual RF carrier time scale differ. This is done to avoid that the RF oscillations would look like a black blur of ink. The RF signal would oscillate about 1,000 times before there would be any noticeable change in the envelope. The ratio between the modulation period and the RF carrier period is artificially lowered for the purpose of visualization. A black-box frequency-domain behavioral model was then extracted based on the measured data. Figure 12 shows the spectral regrowth that is predicted by the model and the spectral regrowth as it was actually measured. As you can see, the correspondence between the modelled and the measured value is very good.

An LSNA instrument must be able to convert the measured wave behavior of a component into a voltage-current representation.

The real beauty of the approach is that it provides much more than just plots of the aforementioned characteristics. The scattering functions can be used in a CAD environment and describe the interdependency between the nonlinear characteristics. As with S-parameters, the scattering

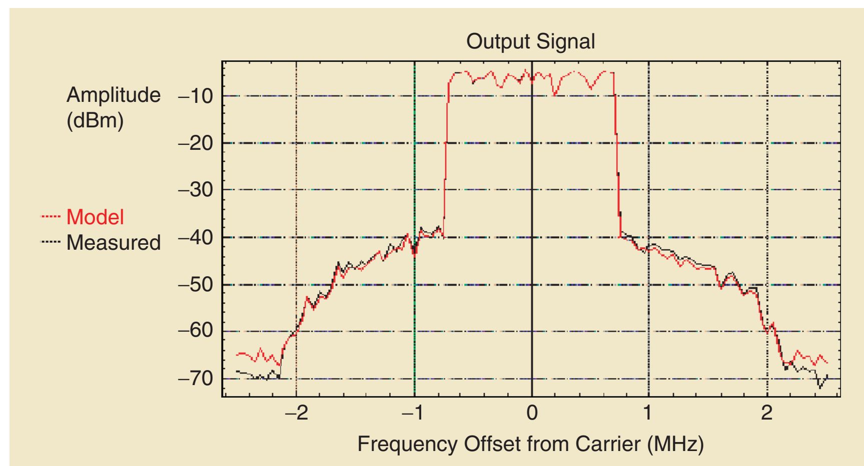

Figure 12. *Modeled and measured spectral regrowth.*

functions approach works both ways. It not only allows for a really accurate automatically extracted CAD model, but it also allows you to experimentally verify the large-signal behavior of a component once it has been designed. A nice characteristic of the scattering functions is that they reduce to classic S-parameters for small input amplitudes. As such, the measurement capability of an LSNA instrument equipped with the means to measure the scattering functions performs a superset of the measurements that are possible with a classic VNA. As such, LSNA instruments will gradually replace all VNAs that are used today to characterize semiconductor devices, easily a multimillion dollar business.

Conclusions

The dream of accurate and complete large-signal characterization of components under realistic operating conditions is made real. The only limit to the scope of applications is the imagination of the R&D people who have access to this measurement capability. LSNA instrumentation and scattering functions are powerful concepts. The associated technology is emerging and will revolutionize the way microwave semiconductor components will be characterized in the future.

Acknowledgments

I would like to thank Larry Dunleavy of Modelithics for reviewing the manuscript and the ARFTG organization (www.arftg.org) for the continued support to the LSNA community. The copyright of the figures and part of the text is with Agilent Technologies (1998), the figures and text are used with permission.

References

[1] R. Marks and D. Williams, "A general waveguide circuit theory," *J. Res. Nat. Inst. Standards Technols.*, vol. 97, pp. 533–562, Sep./Oct. 1992.

[2] M. Sippilä, K. Lehtinen, and V. Porra, "High-frequency periodic time domain waveform measurement system," *IEEE Trans. Microwave Theory Tech.*, vol. 36, pp. 1397–1405, Oct. 1988.

[3] J. Verspecht, "The return of the sampling frequency convertor," in *62nd ARFTG Conf. Dig.*, Boulder, CO, Dec. 2003. [Online] Available: http://www.janverspecht.com

[4] J. Verspecht, "Broadband sampling oscilloscope characterization with the 'nose-to-nose' calibration procedure: A theoretical and practical analysis," *IEEE Trans. Instrum. Meas.*, vol. 44, pp. 991–997, Dec. 1995. [Online] Available: http://www.janverspecht.com

[5] D.F. Williams, P.D. Hale, T.S. Clement, and J.M. Morgan, "Calibrating electro-optic sampling systems," in *Int. Microwave Symp. Dig.*, Phoenix, AZ, May 20–25, 2001, pp. 1527–1530.

[6] J. Verspecht and D. Schreurs, "Measuring transistor dynamic loadlines and breakdown currents under large-signal high-frequency operating conditions," in *1998 IEEE MTT-S Int. Microwave Symp. Dig.*, June 1998, vol. 3, pp. 1495–1498.

[7] D. Schreurs, J. Verspecht, B. Nauwelaers, A. Barel, and M. Van Rossum, "Waveform measurements on a HEMT resistive mixer," in *47th ARFTG Conf. Dig.*, June 1996, pp. 129–135.

[8] J.B. Scott, J. Verspecht, B. Behnia, M. Vanden Bossche, A. Cognata, F. Verbeyst, M.L. Thorn, and D.R. Scherrer, "Enhanced on-wafer time-domain waveform measurement through removal of interconnect dispersion and measurement instrument jitter," *IEEE Trans. Microwave Theory Tech.*, vol. 50, pp. 3022–3028, Dec. 2002.

[9] D. Barataud, F. Blache, A. Mallet, P.P. Bouysse, J.-M. Nébus, J.P. Villotte, J. Obregon, J. Verspecht, and P. Auxemery, "Measurement and control of current/voltage waveforms of microwave transistors using a harmonic load-pull system for the optimum design of high efficiency power amplifiers," *IEEE Trans. Instrum. Meas.*, vol. 48, pp. 835–842, Aug. 1999.

[10] D. Schreurs, J. Verspecht, S. Vandenberghe, and E. Vandamme, "Straightforward and accurate nonlinear device model parameter-estimation method based on vectorial large-signal measurements," *IEEE Trans. Microwave Theory Tech.*, vol. 50, pp. 2315–2319, Oct. 2002.

[11] J. Wood, D.E. Root, and N.B. Tufillaro, "A behavioral modeling approach to nonlinear model-order reduction for RF/microwave ICS and systems," *IEEE Trans. Microwave Theory Tech.*, vol. 52, pp. 2274–2284, Sep. 2004.

[12] D. Schreurs, S. Vandenberghe, J. Verspecht, B. Nauwelaers, and A. Van de Capelle, "Direct extraction of the nonlinear hemt model from vectorial large-signal measurements," in *Proc. Int. Workshop Advanced Black-Box Techniques Nonlinear Modeling*, Belgium, July 1998, pp. 228–233.

[13] J. Verspecht and P. Van Esch, "Accurately characterizing hard nonlinear behavior of microwave components with the nonlinear network measurement system: Introducing 'nonlinear scattering functions'," in *Proc. Fifth Int. Workshop Integrated Nonlinear Microwave Millimeterwave Circuits*, Germany, Oct. 1998, pp. 17–26.

[14] U. Lott, "Measurement of magnitude and phase of harmonics generated in nonlinear microwave two-ports," *IEEE Trans. Microwave Theory Tech.*, vol. 37, pp. 1506–1511, Oct. 1989.

[15] G. Kompa and F. van Raay, "Error-corrected large-signal waveform measurement system combining network analyzer and sampling oscilloscope capabilities," *IEEE Trans. Microwave Theory Tech.*, vol. 38, pp. 358–365, Apr. 1990.

[16] F. van Raay and G. Kompa, "A new on-wafer large-signal waveform measurement system with 40 GHz harmonic bandwidth," in *1992 IEEE MTT-S Int. Microwave Symp. Dig.*, 1992, vol. 3, pp. 1435–1438.

[17] M. Demmler, P.J. Tasker, and M. Schlechtweg, "On-wafer large signal power, S-parameter and waveform measurement system," in *Conf. Rec. Third Int. Workshop Integrated Nonlinear Microwave Millimeterwave Circuits*, Duisburg, Germany, Oct. 1994, pp. 153–158.

[18] J.G. Leckey, J.A.C. Stewart, A.D. Patterson, and M.J. Kelly, "Nonlinear MESFET parameter estimation using harmonic amplitude and phase measurements," in *1994 IEEE MTT-S Int. Microwave Symp. Dig.*, May 1994, vol. 3, pp. 1563–1566.

[19] C.J. Wei, Y.A. Tkachenko, J.C.M. Hwang, K.E. Smith, and A.H. Peake, "Internal-node waveform probing of MMIC power amplifiers," in *IEEE 1995 Microwave Millimeter-Wave Monolithic Circuits Symp.*, May 1995, pp. 127–130.

[20] J. Verspecht, P. Debie, A. Barel, and L. Martens, "Accurate on wafer measurements of phase and amplitude of the spectral components of incident and scattered voltage waves at the signal ports of a nonlinear microwave device," in *1995 IEEE MTT-S Int. Microwave Symp. Dig.*, May 1995, vol. 3, pp. 1029–1032.

[21] C. Arnaud, D. Barataud, J.-M. Nebus, J.-P. Teyssier, J.-P. Villotte, and D. Floriot, "An active pulsed RF and pulsed dc load-pull system for the characterization of power transistors used in coherent radar and communication systems," in *2000 IEEE MTT-S Int. Microwave Symp. Dig.*, June 2000, vol. 3, pp. 1463–1466.

[22] J. Verspecht, F. Verbeyst, and M. Vanden Bossche, "Measurement based behavioural modeling of components under modulated large-signal operating conditions," in *Proc. 30th European Microwave Conf.*, France, Oct. 2000, pp. 369–373.

[23] K.A. Remley, "The impact of internal sampling circuitry on the phase error of the nose-to-nose oscilloscope calibration," NIST Tech. Note 1528, Aug. 2003.

[24] J. Verspecht, D.F. Williams, D. Schreurs, K.A. Remley, M.D. McKinley, "Linearization of large-signal scattering functions," *IEEE Trans. Microwave Theory Tech.*, vol. 53, pp. 1369–1376, Apr. 2005.

[25] D.E. Root, J. Verspecht, D. Sharrit, J. Wood, and A. Cognata, "Broad-band poly-harmonic distortion (PHD) behavioral models from fast automated simulations and large-signal vectorial network measurements," *IEEE Trans. Microwave Theory Tech.*, vol. 53, pp. 3656–3664, Nov. 2005.